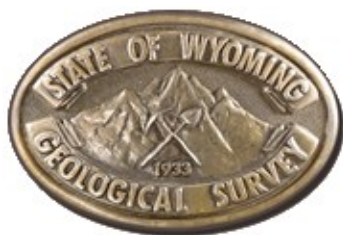


Interpreting the past, providing for the future

Report on the Preliminary Geologic Maps of the Shamrock Hills and Rawlins Peak SW Quadrangles, Carbon County, Wyoming

By Christopher J. Carroll, Ranie M. Lynds, Deirdre R. Ratigan,
and Martin J. Palkovic

Open File Report 15-8
September 2015



Interpreting the past, providing for the future

Wyoming State Geological Survey
Thomas A. Drea, Director and State Geologist

Report on the Preliminary Geologic Maps of the Shamrock Hills and Rawlins Peak SW Quadrangles, Carbon County, Wyoming

By Christopher J. Carroll, Ranie M. Lynds, Deirdre R. Ratigan,
and Martin J. Palkovic

Open File Report 15-8
Wyoming State Geological Survey
Laramie, Wyoming: 2015

To accompany WSGS Open File Reports 15-6 and 15-7

For more information on the WSGS, or to download a copy of this Open File Report, visit www.wsgs.wyo.gov or call 307-766-2286

This Wyoming State Geological Survey (WSGS) Open File Report is preliminary and may require additional compilation and analysis. Additional data and review may be provided in subsequent years. The WSGS welcomes any comments and suggestions on this research. Please contact the WSGS at 307-766-2286, or email wsgs-info@wyo.gov.

Suggested citation: Carroll, C.J., Lynds, R.M., Ratigan, D.R., and Palkovic, M.J., 2015, Report on the preliminary geologic maps of the Shamrock Hills and Rawlins Peak SW quadrangles, Carbon County, Wyoming: Wyoming State Geological Survey Open File Report 15-8, 33 p.

Table of Contents

Introduction.....	1
Location.....	1
Geologic Setting.....	2
Structure.....	3
Fractures.....	4
Economics.....	4
Petroleum.....	5
Coal.....	5
Uranium.....	6
Industrial Minerals.....	6
Alluvial sand and gravel.....	6
Terrace sand and gravel.....	6
Windblown sand.....	7
Older sand and gravel.....	7
Bentonite.....	7
Description of Map Units.....	7
Cenozoic Deposits and Sedimentary Rocks.....	7
Quaternary.....	7
Paleogene.....	9
Mesozoic Sedimentary Rocks.....	11
Cretaceous.....	11
References.....	20
Appendix A: Detrital Zircon Geochronology.....	24
Appendix B: Palynology.....	28
Previous Investigations.....	28
Methods.....	28
Results.....	29
Age.....	29
Paleoenvironment.....	29
Appendix C: Coal Quality.....	31

INTRODUCTION

The Rawlins Peak SW (Carroll and others, 2015) and Shamrock Hills (Lynds and others, 2015) 1:24,000-scale quadrangles are located in south-central Wyoming on the eastern margin of the Great Divide Basin (fig. 1), a sub-basin of the Greater Green River Basin. Barlow (1953) originally mapped the study area as part of a larger study on the Rawlins uplift at the scale of approximately 1:126,720, which was followed by a 1:100,000 Rawlins 30' x 60' quadrangle (McLaughlin and Fruhwirth, 2008). Other mapping in the nearby area includes a 1:12,000-scale map of the Rawlins uplift (Otteman and Snoke, 2005), a 1:100,000-scale map of the Rawlins-Little Snake River area (Hettinger and others, 2008), and a 1:24,000-scale map of the Separation Rim quadrangle (Gregory and Bagdonas, 2012).

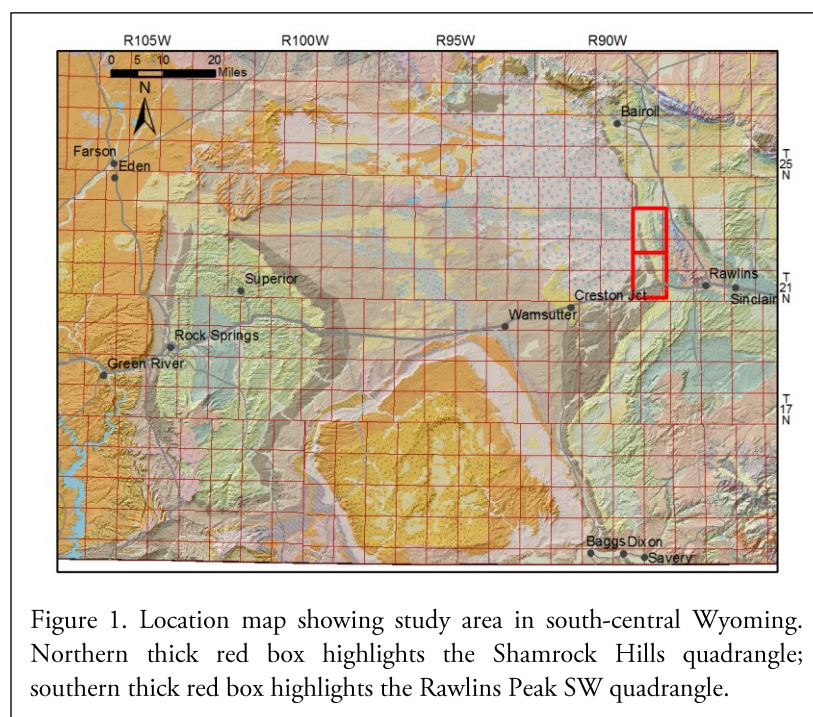


Figure 1. Location map showing study area in south-central Wyoming. Northern thick red box highlights the Shamrock Hills quadrangle; southern thick red box highlights the Rawlins Peak SW quadrangle.

Previous work mapped the study area at low resolution, grouping many of the Upper Cretaceous and Paleocene units. This study distinctly mapped the Mesaverde Group into its respective formations, defined the members of the formations above and below the Cretaceous-Paleogene boundary, and correlated mappable coal beds.

Mapping was conducted through on-the-ground examination and measurement of rock units, aerial imagery interpretation, and compilation of previous mapping and written reports. Field work encompassed more than 52 days for four geologists between September 2014 and August 2015. Mapping

was completed in cooperation with the U.S. Geological Survey 2014 STATEMAP grant award G14AS00006.

We wish to acknowledge and thank the landowners and caretakers for access to their private lands. This project would not have been possible without their generosity.

LOCATION

The Great Divide Basin is a 16,000 km² (6,200 mi²) structural basin bounded on the east by the Rawlins uplift, on the south by the Wamsutter arch, on the west by the Rock Springs uplift, and on the north by faulted uplifts of the Wind River Range and Granite Mountains. The Great Divide Basin lies within the Greater Green River Basin, a 32,000 km² (12,400 mi²) basin containing numerous sub-basins in southern Wyoming. The Great Divide Basin is an endorheic, intermontane desert basin that lies on the continental divide, with an average elevation of 2,100 m (6,900 ft) above sea level (Heller and others, 2011) and annual

average wind speeds of 25 km/hr (16 mi/hr) in summer and 36 km/h (22 mi/hr) in winter (Martner and Marwitz, 1982).

The study area is within Carbon County, Wyoming, and includes all of Rawlins Peak SW and Shamrock Hills 7.5' quadrangles (Tps. 21, 22, and 23 N., Rs. 88 and 89 W.). The eastern edge of the Rawlins Peak SW 7.5' quadrangle is 11 km (7 mi) west of Rawlins. U.S. Interstate 80 (I-80 or Interstate 80) transects the southern portion of the map. The northern map area is accessible via exit 204 Knobs Road, and exit 206 Hadsell Road, from I-80. The southeast corner of the Shamrock Hills 7.5' quadrangle is located approximately 15 km (9 mi) northwest of Rawlins. The quadrangle is accessible from the south via exit 204, Knobs Road on I-80, and from the north by Mineral X road (Carbon County Road 63/BLM Road #3206), from U.S. Highway 287.

Both quadrangles are within the “checkerboard,” an area where ownership alternates every section between privately held land and public land operated primarily by the Bureau of Land Management (in addition to some State of Wyoming sections), resulting in a checkerboard ownership pattern. Permission must be obtained from land owners prior to entering private lands.

GEOLOGIC SETTING

The Upper Cretaceous through Eocene strata exposed within the study area record the retreat of the Western Interior Seaway and a transition to wholly non-marine intrabasinal sedimentation. During deposition of the oldest mapped unit, the Upper Cretaceous Steele Shale, through deposition of the Upper Cretaceous Fox Hills Sandstone and parts of the lower member of the Lance Formation, the study area was in the foreland basin of the Sevier orogenic belt, on the western margin of the resultant Western Interior Seaway. Sea level regression was recorded by the transition from the Steele Shale through the Haystack Mountains and Allen Ridge Formations. This regression was capped by the fluvial Pine Ridge Formation, whose base is unconformable, suggesting a regional drop in sea level. Sea level transgression began during Almond Formation time, and was at its deepest during deposition of the Lewis Shale. Regression was renewed during Fox Hills Sandstone and lower Lance Formation time.

The Laramide orogeny commenced during the Late Cretaceous, most notably within the study area during deposition of the Red Rim Member of the Lance Formation. This period of mountain building, responsible for much of the present geometry of the Great Divide Basin and the basin-margin uplifts, also resulted in basin subsidence. The Late Cretaceous to late Paleocene was a time of continued deposition, and the Greater Green River Basin was connected to other basins farther east such as the Hanna, Carbon, and Laramie basins (Lillegraven, 2015). During the transition from the Cretaceous to the Paleogene (Tertiary), the Western Interior Seaway had retreated to the northeast and the subsiding Great Divide Basin began accumulating Paleocene sediments of the coal-bearing Fort Union Formation. Subsidence continued into the Eocene and was likely tapering off during deposition of the Battle Spring Formation, an alluvial fill derived from the Granite Mountains to the north. Intrabasinal faults common in the two map areas extending outward from the Rawlins uplift may suggest basement block fault movements (Lillegraven, 2015).

Regional uplift and erosion during the Neogene removed thousands of meters of sediments and resulted in the high elevations and rock exposures displayed today. These outcrops were then eroded, reworked, and deposited as silt, sand, and gravel in the form of alluvium, colluvium, sand dunes, loess, pediment gravels, and terrace gravels during the Quaternary. Marrs and Grasso (1991) proposed the existence of Lake Wamsutter, a

large lake that filled much of the northern Great Divide Basin, during the Pleistocene. Separation Flats was a natural spillway from Lake Wamsutter, resulting in a fluvio-lacustrine alluvial plain. Today, Separation Flats is a sparsely vegetated region of unconsolidated clay, silt, and sand reworked and added to by Holocene alluvial and eolian processes.

STRUCTURE

The Greater Green River Basin is a large Laramide basin encompassing a series of sub-basins. The Great Divide Basin, the northeast sub-basin, is mostly a flat-lying sedimentary sequence with steeply dipping Cretaceous and Paleocene rocks along the margin. Within the study area, these basin-margin strata dip to the west. The outcrops trend north-northwest to south-southeast, with slight changes in strike suggestive of gentle folding, including a syncline mapped within the Cretaceous rocks at T. 22 N., R. 89 W., sec. 25, and T. 22 N., R. 88 W., sec. 30.

The most prominent structural feature in the region is the Rawlins uplift, a structurally complex asymmetric anticline with Precambrian rock exposed in the center, surrounded by hogbacks of Mesozoic strata, and bounded on the west by a series of thrust faults just east of the study area. The main thrust fault, responsible for 8,200 m (27,000 ft) of displacement between the basin and the core of the uplift, is a subsurface low-angle fault that dips to the east (Otteman and Snoke, 2005). The Belle Springs Fault, exposed at the surface east of the study area (Barlow, 1953), is a splay from the master fault (Otteman and Snoke, 2005). A broad and gentle anticline in the Steele Shale (and Niobrara Formation?), west of the Belle Springs Fault, is the result of this faulting. Although exposure is poor, the few outcrops available suggest dips change from approximately 50° west-southwest in the Haystack Mountains Formation to less than 15° in the eastern-most exposures of the Steele Shale.

The southern part of the study area hosts a large southeast-northwest asymmetric syncline with a fold axis approximately paralleling Interstate 80 and the Union Pacific Railroad tracks. On the southern limb of the syncline, strata dip 4°–17° northwest, while beds on the north side of the syncline dip 63°–72° southwest. The syncline is faulted along the center axis at T. 21 N., R. 89 W., sec. 19. The fault, trending approximately 300°, is a dividing point between two distinct structural domains. Some authors have even suggested that this zone is part of a larger regional thrust fault deeper in the subsurface, but bedrock mappers in the area have interpreted this feature as an asymmetric syncline that plunges in a northwesterly direction. Folding probably occurred during the late Paleocene or early Eocene (Dames & Moore Co., 1978). Another fault offsetting steeply dipping beds on the north limb of this syncline is a right-lateral oblique-slip fault that trends 195° in T. 21 N., R. 89 W., sec. 7. This fault offsets beds of the Fox Hills Sandstone, Lewis Shale, and the Dad Sandstone Member of the Lewis Shale, and is interpreted with some normal displacement.

A series of faults located along the Rawlins Peak SW and Shamrock Hills quadrangle boundary offset the Mesaverde Group and the Steele Shale. The southernmost—and largest—of these faults is mapped as left-lateral to normal oblique-slip, trending approximately 210°. Smaller and sub-parallel left-lateral oblique-slip faults are mapped north of this main fault, as well as a conjugate right-lateral oblique-slip fault, trending 120°, that offsets the Pine Ridge Sandstone and Almond Formation in T. 22 N., R. 89 W., secs. 13 and 14. These faults are probably related to subsidence of the Rawlins uplift in post-Miocene time (Barlow, 1959).

Two lineaments that may be faults as well were mapped within the study area. The northernmost lineament trends 030° from T. 23 N., R. 89 W., sec. 33 to T. 23 N., R. 89 W., sec. 26. This lineament is on trend with

the fault that defines the northern boundary of the Rawlins uplift, suggesting possible normal displacement with the northern block down dropped relative to the southern block. Further evidence for faulting is discernable from the topography: Shamrock Draw originates in T. 22 N., R. 89 W., sec. 11, tracks northwest to T. 23 N., R. 89 W., sec. 27, then abruptly turns northeast and crosses the Mesaverde Group outcrops of the Shamrock Hills proper. This lineament is likely tied to a larger lineament or fault, although no displacement was observed during field mapping. The second lineament is mapped in T. 22 N., R. 89 W., secs. 1 and 12. No field evidence for faulting was observed from this lineament, but the lineament may be indicative of the structural complexities that likely occur within the Steele Shale and are not mappable due to poor exposure.

Within the study area, there is evidence that basin-margin deformation began during the Paleocene and continued into the Eocene. Specifically, there is approximately a 30° dip change from about 55° to the west-southwest in most of the Cretaceous as well as the Paleocene China Butte Member of the Fort Union Formation, to 20° west-southwest in the Overland Member of the Fort Union Formation. The overlying Eocene Battle Spring Formation onlaps onto—and in the north completely covers—the Overland Member, with dips of approximately 15°–20° west.

Fractures

Sandstone joints and coal cleat measurements of the Fort Union Formation, Lance Formation, and Mesaverde Group all show fracture orientations that reflect a complex history of Laramide and post-Laramide structural events. Grout and Verbeek (1992) identified seven sets of extension joints on the Rawlins uplift, but only three sets were observed during field mapping. These fractures form large, prominent joints in the sandstones, expressed as planar surfaces with very small apertures and spacing ranging from 0.2 m (0.7 ft) to 2 m (6.6 ft). These fractures are usually through-going but terminate as hairline cracks. Most of the fractures are open-mode type with limonite and pyrite crystals and occasional calcite filling of coal cleats. Station 17 from Grout and Verbeek (1992) is located on Rawlins Peak SW quadrangle, and indicates two Mesaverde Group fractures (F5 and F6) with orientations of 067° and 331°, respectively. These are considered two of the youngest regional joint sets in the Mesaverde Group rocks of the Great Divide Basin.

Several fractures measured for this study on the Rawlins Peak SW quadrangle indicate China Butte sandstones with a main J1 fracture orientation of 040°, dipping 82° southeast, and a J2 subsequent set of 275°, dipping 72° north. Fracture development in the Fox Hills Sandstone and lower member of the Lance Formation shows J1 fractures approximately striking 252°, dipping 72° northwest, and J2 fractures striking 022°, dipping 21° southeast. These measurements, while different than Grout and Verbeek (1992), indicate that local extension features vary from one unit to the next, based on differing rock properties.

ECONOMICS

Exploration and exploitation of coal, natural gas, and uranium resources in the Great Divide Basin west of the map area highlight an economic interest in these energy-producing resources in the Battle Spring Formation, Fort Union Formation, and Mesaverde Group. These maps extend the coal resource maps of Hettinger and others (2008) from the Atlantic Rim northward through the Rawlins Peak SW quadrangle, denote petroleum exploration within the study area, emphasize possible subsurface petroleum reservoirs through detailed outcrop mapping, and describe areas of potential industrial mineral accumulations.

Petroleum

Historical petroleum development from nearby structures targeted the geologic formations underlying these quadrangles. The earliest petroleum discovery in the area was the Lost Soldier field in 1916, 58 km (36 mi) northwest of Rawlins and 27 km (17 mi) north of the northern boundary of the study area. Production was initially from the Pennsylvanian Tensleep Sandstone.

Parts of the Bell Springs field are located within the study area, in the extreme northeast corner of the Shamrock Hills quadrangle, T. 23 N., R. 88 W. It is a dome-like feature located west of the Bell Springs Fault (Krampert, 1951). Discovered in 1924, the Belle Springs field is currently abandoned, with production last reported in 1987 totaling 2,719,128 Mcf natural gas and no oil (WOGCC, 2015). The field consists of 21 permanently abandoned wells that produced from the Canyon Springs, Cloverly, Frontier, and Sundance Formations (WOGCC, 2015). Oil and gas exploration has not occurred in the Rawlins Peak SW quadrangle.

The Paleocene and Upper Cretaceous strata of the Greater Green River Basin are of exploration interest to numerous petroleum companies. Natural gas in low-permeability sandstone reservoirs and coalbed methane gas are targets in these formations in the Washakie and Great Divide Basins, and especially on the nearby Wamsutter arch. However, the steep dip of these formations in the majority of the study area limits the potential for gas trapping, and thus exploration.

Coal

Coal-bearing formations in the Shamrock Hills and Rawlins Peak SW quadrangles include the Fort Union, Lance, Almond, and Allen Ridge Formations. Subbituminous coal and lignite are found in the China Butte Member of the Fort Union Formation. The Rawlins Peak SW quadrangle lies at the northern boundary of



Figure 2. Coal sampling within the China Butte Member of the Fort Union Formation.

the Little Snake River coal field. Various authors have studied the coal resources in the area including on the Riner (Sanders, 1974) and Creston Junction (Sanders, 1975) quadrangles, on the Seaverson Reservoir quadrangle (Edson, 1979), and in the Fort Union Formation south of Interstate 80 (Hettinger and others, 2008). Dames & Moore Co. compiled coal information for Riner (1979) and Rawlins Peak SW (1978) quadrangles, but did not include original mapping. Subsurface geologic data for coal exploration was provided by the Rocky Mountain Energy Co. (2014), and the U.S. Geological Survey drilling and reconnaissance mapping. Coal bed names were adopted on the Rawlins Peak SW quadrangle and extrapolated northward after Hettinger and others (2008).

Outcrop coal quality sampling of 15 coal bed locations in the Rawlins Peak SW quadrangle (fig. 2) show that the Fort Union Formation samples are characterized as low sulfur, moderate ash, sub-bituminous coal (Appendix C). The average ash content of outcrop sampling is 8.6 percent (as-received), heating value (7,468 Btu—low value due to weathered coal), 0.3

percent sulfur, and 0.05 mg/kg mercury. Moisture (21.6 percent), volatile matter (34.1 percent), and fixed carbon (38.2 percent) all were typical of subbituminous coal values for the area.

Fort Union Formation coal resource calculations by Dames & Moore Co. (1978) for Rawlins Peak SW assumed subbituminous coal (1,770 short tons per acre-ft). Federal coal sections total 46 million short tons from four mineable Fort Union Formation coal beds. Of this amount, 37 million short tons are considered underground mineable and 9 million short tons are potentially surface mineable (Dames & Moore Co., 1978). The Shamrock Hills quadrangle has a lesser volume and steeper dip of coal within its units that warrant unmineable conditions, and was not mapped by Dames & Moore Co., or as part of this study.

One active permitted coal project (DEQ-LQD - RD0017) is located on the Rawlins Peak SW quadrangle at T. 21 N., R. 89 W, secs. 11 and 12. This is the Carbon County UCG site for coal gasification. It is a U.S. Department of Energy research and development site that has tested the underground coal gasification potential of the Fort Union Formation coal beds since 1983 (Saracino, 1984). The main coal bed was measured at 9.5 m (31 ft) thick, but may reflect an apparent thickness. This site is now in air-sparging remediation for closure.

Uranium

The Eocene Battle Spring Formation is a spatially expansive uranium-bearing unit that is exposed throughout most of the Great Divide Basin, and exists on the west side of the study area. Uranium is mined from the Battle Spring Formation nearby in the Great Divide Basin, including Ur-Energy's Lost Creek in-situ recovery mine, but is not known to exist within the study area. Uraniferous coal beds have also been described in the central (Pipiringos, 1961) and east-central (Masursky, 1962) Great Divide Basin. Uraniferous coals occur in the Eocene Wasatch and Battle Spring Formations, as well as in the upper Fort Union Formation. Masursky (1962) suggests that Fort Union coal beds west of the Rawlins uplift (and presumably located within the study area) "are locally uranium bearing." Coal-bearing uraniumiferous coals were identified in drill holes 20 km (12 mi) west of the Rawlins Peak SW quadrangle (Masursky, 1962).

Industrial Minerals

The study area does not have abundant industrial minerals, but does have a few deposits worth noting, as defined by Harris (2004).

Alluvial sand and gravel

Located along and adjacent to Separation Creek, alluvial sand and gravel consists of intermittent stream deposits containing clasts that range in size from silt to gravel, locally interbedded with clay (Harris, 2004). These deposits are correlative to alluvium (Qal) and alluvium and colluvium, undivided (Qac), mapped on the Shamrock Hills and Rawlins Peak SW quadrangles, respectively.

Terrace sand and gravel

Harris (2004) defines terrace sand and gravel as Quaternary/Tertiary terrace gravels. These correlate to the pediment deposits (QTp) on the northeast and east side of the Shamrock Hills quadrangle. No pediment deposits were observed on the Rawlins Peak SW quadrangle.

Windblown sand

Windblown sand includes both active (unstabilized) and stabilized sand dunes and deposits (Harris, 2004). These correlate to the sand and loess (Qs) mapped on both the Shamrock Hills and Rawlins Peak SW quadrangles. Windblown sand may be a potential source of sand for hydraulic fracturing used in the petroleum industry, or as a material for the construction industry.

Older sand and gravel

Older sand and gravel consists of poorly consolidated to unconsolidated gravels and conglomerates (Harris, 2004). Within the study area, this corresponds to the mapped terrace and other gravels (QTg) and the Battle Spring Formation (Tbs).

Bentonite

One bentonite marker bed approximately 0.6–0.9 m (2–3 ft) thick was mapped in the Lewis Shale within the Rawlins Peak SW quadrangle, south of Indian Springs Creek. This bentonite bed was not observed on the Shamrock Hills quadrangle. Finn and Johnson (2005) show another bentonite bed, termed the “Asquith marker,” in the Great Divide Basin west of the map area. The Asquith marker is in the lower Lewis Shale, below the Dad Sandstone Member. This bentonite was not observed within the study area, most likely due to poor exposure.

DESCRIPTION OF MAP UNITS

Cenozoic Deposits and Sedimentary Rocks

Quaternary

Artificial fill (af)

Artificial fill consists of clay, silt, sand, gravel, cobbles, and boulders derived from surrounding Quaternary deposits and bedrock. Artificial fill is used in railroad and highway grades, and to a lesser extent in small embankment dams and stock ponds, where it is less than 24 m (79 ft) thick. Fill material is only mapped where it is greater than 1.5 m (5 ft) thick.

Playa lake deposits (Qpl)

Dry playa lake deposits are comprised of unconsolidated to well-consolidated clay and silt. Vegetation is sparse and generally limited to sagebrush. Mud cracks are most common in the topographically lowest areas. Material derived from Separation Creek flows into an undrained depression on the northwest part of Shamrock Hills quadrangle. The thickness of playa lake deposits could not be determined from field relations.

Sand and loess (Qs)

Stabilized sand dunes, loess, and general wind-transported clay and silt are common in the study area. These wind-blown units are distinctly vegetated and can fully obscure the bedrock beneath them. A maximum thickness of approximately 5 m (16 ft) is reached near Separation Creek at the border between the Shamrock Hills and Rawlins Peak SW quadrangles.

Alluvium (Qal)

Alluvium in the map area consists of unconsolidated to poorly consolidated clay, silt, sand, gravel, and cobbles, mainly along intermittent stream courses and in floodplains. The alluvial material is derived from all local geologic units, and comprises all of Separation Flats as well as Separation Creek and other minor ephemeral tributaries. All mapped fluvial material is derived from the Rawlins uplift area and drains westward into Separation Creek. The alluvium of Separation Flats marks the spillover of former Lake Wamsutter (Marrs and Grasso, 1991), and is only mapped on the Shamrock Hills quadrangle. Alluvium generally ranges from 0–8 m (26 ft) in thickness.

Alluvium and colluvium, undivided (Qac)

Undivided alluvium and colluvium is mapped at the base of slopes and along some intermittent streams. It consists of unconsolidated to poorly consolidated clay, silt, sand, and gravel. The alluvium and colluvium are derived from local geologic units, and are often capped by a thin veneer of clay-rich soil. Slope wash, small talus slopes, and small alluvial fans are also included as part of alluvium and colluvium. Thickness is generally less than 5 m (16 ft).

Terrace gravels (Qtg)

Terrace gravels consist of light- to dark-brown, orangish-brown, yellowish-gray, gray, and black, unconsolidated subangular to subrounded pebble gravel derived from local Cretaceous and Paleogene bedrock along Separation and Fillmore Creeks. Clasts are up to 8 cm (3 in) in diameter. The unit is 2–15 m (7–49 ft) above creek level and approximately 0–10 m (0 ft) thick.

Pediment deposits (QTp)

Pediment deposits are smooth surfaces that gently dip to the west. Pediments are comprised of unconsolidated subangular to subrounded clasts derived from the Rawlins uplift (fig. 3), as well as other metamorphic clasts of unknown origin, in a coarse sandy matrix. Clast size ranges from pebbles to boulders. Pediment deposits are only found on the east side of the Shamrock Hills quadrangle and are less than 3 m (10 ft) thick.



Figure 3. Pediments derived from the Rawlins uplift in the background (photo looking east).

Terrace and other gravels (QTg)

Terrace deposits are located on planar erosional surfaces along rivers and streams. Terrace deposits consist of unconsolidated to locally cemented silt, sand, gravel, cobbles, and boulders of igneous and metamorphic origin located adjacent to intermittent stream courses. The east side of Separation Creek features a possible gravel lag derived from the Battle Spring Formation (fig. 4), while the west side exhibits gravels mixed with locally derived sedimentary rock. Terrace and other gravels are up to 6 m (20 ft) thick.

Paleogene

Battle Spring Formation, Eocene (Tbs)

The Battle Spring Formation is an arkosic conglomerate, sandstone, and siltstone that covers much of the northern Great Divide Basin. Within the study area, the Battle

Spring Formation is medium- to coarse-grained sandstone, with poor sorting and angular clasts. Outcrops generally occur as cross-bedded white to light-gray sandstone that form resistant but friable low-lying pillars and mounds (fig. 5). Resistant outcrops are often clast-supported pebble conglomerates that contain ferruginous concretions up to 0.6 m (2 ft) in diameter. Carbonaceous shale and coal are rare but present (fig. 4). Locally, poor outcrop exposure is usually indicative of siltstone and mudstone that are mappable as grass-covered pink- to buff-colored slopes.

The coarser-grained Battle Spring Formation interfingers with the Eocene Wasatch Formation west of the study area, and is interpreted as being deposited in proximal alluvial fans, river valleys, and deltaic depositional environments derived from the Granite Mountains to the north (Pipiringos, 1955). Pipiringos (1955) suggests the Battle Spring Formation is Eocene based on fossil evidence in the Wasatch Formation and this interfingering relationship. Bilby and others (2010) suggest that part of the Battle Spring Formation mapped along a pipeline trench east of Riner, Wyoming, contains late Paleocene leaf fauna. The correlative area to these rocks is mapped as Fort Union Formation on the Rawlins Peak SW quadrangle.

The Battle Spring Formation lies at an angular unconformity on the Paleocene Fort Union Formation surface. The full thickness of the Battle Spring

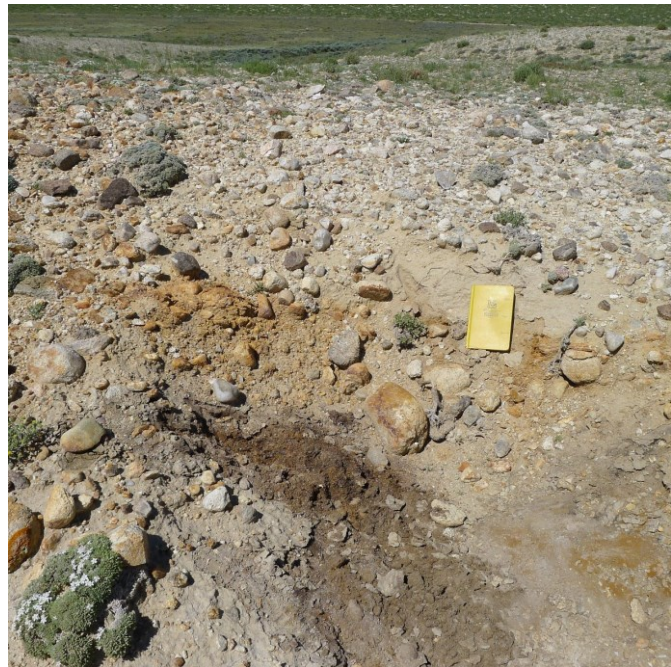


Figure 4. Gravels derived from and capping a carbonaceous zone of the Eocene Battle Spring Formation. Gravels slope west to Separation Creek.



Figure 5. Coarse-grained sandstones from the Battle Spring Formation.

Formation is not exposed within the study area, but is inferred to have a minimum thickness of 1,000 m (3,300 ft) further west in the Great Divide Basin (Pipiringos, 1955).

Fort Union Formation, Paleocene (T_{fo}, T_{fc})

The Fort Union Formation represents a fluvial but low-lying coastal plain depositional environment of Laramide basin fill, and is stratigraphically equivalent to other Paleocene units throughout Wyoming. On the east flank of the Washakie Basin, Honey and Hettinger (2004) formally defined the Overland (youngest) and the China Butte (oldest) Members of the Fort Union Formation, separated by an unconformity. Lynds and Carroll (2015) further extended these correlations into the Great Divide Basin, which were mapped within the study area.

Overland Member (T_{fo}): The upper middle and upper Paleocene Overland Member of the Fort Union Formation of Hettinger and others (2008) is a poorly exposed light-gray sandstone that weathers brown to dark-brown with desert varnish. The sandstones are interbedded with shale and carbonaceous shale. Sandstones are fine- to coarse-grained, moderately to poorly sorted, well indurated, and contain ferruginous concretions up to 0.3 m (1 ft) in diameter.

Near the base of the Overland Member are coarse-grained sandstones with occasional chert pebbles and cross-beds several meters thick. These basal sands correlate with the basal sandstone member defined by Hettinger and others (2008). The upper part of the Overland Member is coal-rich but poorly exposed, and hosts the Cherokee coal zone (labeled T_{foc} on Hettinger and others, 2008) found on the Riner quadrangle (Sanders, 1974), but is not exposed within the map area.

The basal contact is sharp and unconformable, with a decrease in dip from the underlying China Butte Member of approximately 35°. The upper contact is also sharp and unconformable, overlain by the Battle Spring Formation. The maximum exposed thickness within the study area is approximately 550 m (1,800 ft) on Shamrock Hills quadrangle, but nearby subsurface thickness is approximately 700 m (2,300 ft) (Lynds and Carroll, 2015).

China Butte Member (T_{fc}): The China Butte Member of the Fort Union Formation consists of fine- to medium-grained, moderately well-sorted, subangular, white to gray lenticular sandstone that weathers white to light brown. Ferruginous concretions and iron oxide limonite staining on bedding surfaces are common. Sandstones are interbedded with shale, carbonaceous shale, and subbituminous coal. The upper part contains a higher density of resistant sandstone lenses with crayfish burrows (fig. 6) (Hasiotis and Honey, 2000) interbedded with coal and carbonaceous shales (fig. 7A). The lower 250 m (820 ft) section is a thick coal-bearing zone (fig. 7B) (Lynds and Carroll, 2015), but is mostly covered on the north end of the study area. Coaly units generally contain alternating beds of subbituminous black coal and brown to dark-brown carbonaceous shale over a 1.5–9.1 m (5–30 ft) thick zone.

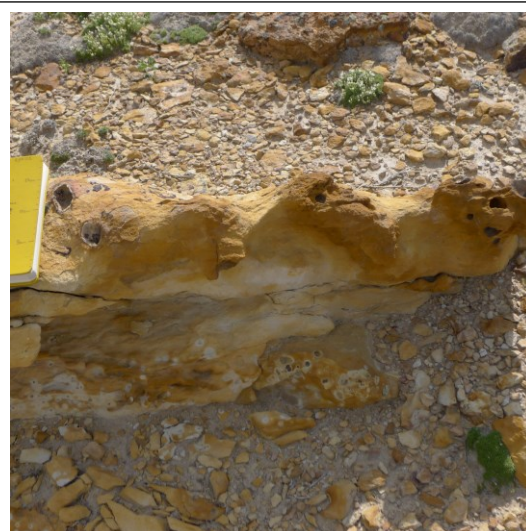


Figure 6. Crayfish burrows preserved in a thin sandstone lens near the top of the China Butte Member of the Fort Union Formation.



Figure 7. Typical outcrops from the China Butte Member of the Fort Union Formation showing (A) interbedded sandstone, shale, and carbonaceous shale (looking southwest) and (B) the China Butte coal zone on the Rawlins Peak SW quadrangle (looking west).

On the Rawlins Peak SW quadrangle, the uppermost exposed coals, first delineated by Hettinger and Brown (1979), correlate to the Chicken Springs, Fillmore Ranch, and Fillmore Creek coal zones of Hettinger and others (2008). The mid-section part of the coal-bearing interval containing coal beds correlative to the Muddy Creek, Separation Creek B, and Riner coal beds of Hettinger and others (2008) are only present in the southern half of the quadrangle, and are not laterally continuous. The lower part of the coal-bearing interval contains thick and laterally extensive coal beds (correlated after Hettinger and others, 2008) including the Lower Riner, Olson Draw, Lower Olson Draw, Hadsell Draw, and Red Rim coal zones. The Red Rim coal zone averages 2.4 m (7.9 ft) thick with carbonaceous shale, mudstone roof rock, and sandstone floor rock, a maximum apparent thickness of 9.5 m (31 ft) (G coal of Saracino, 1984) north of Interstate 80, and is the main target for an underground coal gasification pilot study at NE¼SE¼ sec. 11, T. 21 N., R. 89 W. The lowermost coal is the Daley Ranch, found only in the southern part of the Rawlins Peak SW quadrangle.

The base of the China Butte Member is characterized by a 1.2 m-thick (3.9 ft) pebble conglomerate and sandstone in a very dark, coarse-grained, iron-oxide cemented matrix. Clasts are gray and black chert. This unit is only observed south of the Union Pacific Railroad tracks on the south end of the study area. The China Butte Member is considered a continental to fresh-water coastal plain facies that is approximately 900 m (2,900 ft) thick. The basal contact with the Red Rim Member of the Lance Formation is sharp and unconformable.

Mesozoic Sedimentary Rocks

Cretaceous

Lance Formation (Klr, Kll)

The Lance Formation was subdivided by Honey and Hettinger (2004) into the upper Red Rim Member and the lower (unnamed) member.

Red Rim Member (Klr): Also called the Unnamed Cretaceous sandstone unit (Hettinger and Kirschbaum, 1991), the Unnamed Cretaceous and Tertiary sandstone unit (Hettinger and Kirschbaum, 1991; Hettinger

and others, 1991), and the Massive K/T Sandstone (Tyler and others, 1995), this prominent thick sandstone extends throughout the Rawlins Peak SW quadrangle and the southern two-thirds of the Shamrock Hills quadrangle, as distinct sandstone fins overlain by 15 m (50 ft) of brown iron-stained sandstone. Appendix B contains a summary of palynology work conducted in this area.

The member contains fine- to medium-grained, some coarse-grained, moderately to well-sorted, subangular white to light-gray tabular cross-bedded quartz sandstone that may weather orangish-red (fig. 8). South of Interstate 80, the color changes to reddish-brown. Beds of poorly sorted, subangular, coarse-grained sandstone to pebble conglomerate are 61 m (200 ft) below the top of the unit. Red, black, yellow, gray, and translucent subangular chert clasts, with salt and pepper texture, occasional honeycomb weathering, and ferruginous concretions up to 0.3 m (1 ft) in diameter can be found throughout the unit. Pebble conglomerate



Figure 8. Outcrops of the Red Rim Member of the Lance Formation north of Interstate 80.

beds also have associated mud rip-ups, carbonaceous clasts, woody material, and chert pebbles. On the quadrangle the uppermost 15 m (49 ft) contains brown iron-stained sandstone. The middle of the member crops out as distinct sandstone fins with more than 15 m (49 ft) of relief, and slump structures and faint bedding are common. The basal contact is sharp but conformable, and the Cretaceous-Paleogene boundary is likely at or near the upper contact (Hettinger and others, 2008). The Red Rim Member is considered fluvial sandstone of higher energy than the overlying China Butte Member of the Fort Union Formation. It thins from 120 m (390 ft) in the southern study area to zero on the northern part of the Shamrock Hills quadrangle.

Lower Member (KII): The lower (unnamed) member of the Lance Formation consists of fine-grained, well-sorted, well-rounded rusty brown and light-tan dune and ripple-scale cross-bedded sandstone, interbedded with dark-brown shale and lesser carbonaceous shale and coal. The upper zone of the lower Lance member, as defined by Lynds and Carroll (2015), is marked by a poorly exposed shale valley throughout most of the study area. The lower zone consists of dark sandy to silty shale with multiple beds of thin to thick sandstone that comprise more than 50 percent of the section (fig. 9). Potassium feldspar and black lithic grains are commonly observed in sandstones. The beds average 2 m (6.5 ft) thick but range 0.3–10 m (1–33 ft), can contain a rusty brown diagenetically altered zone at the top, and persist laterally for a few hundred to a few thousand meters. Shell fragments are found throughout the lower zone and include mollusks *Plesielliptio* sp. and *Proparveysia* sp., as well as other unidentified unionids and possible *Tylostoma?* sp. (Hartman and others, 2015; and J. Hartman, written commun., 2015). *Ophiomorpha* trace fossils are found rarely in the lowest 300 m (980 ft) of section. Coal and carbonaceous shale are more common near the base, which is gradational and conformable. One coal bed observed in a canyon in NW $\frac{1}{4}$ NE $\frac{1}{4}$ sec. 12, T. 21 N., R. 89 W., was 2.7 m (8.9 ft) thick. This lower member represents a low energy coastal plain to marginal marine facies that interfingers with the Fox Hills Sandstone at the base. Thickness of the lower member ranges approximately 1,130–1,400 m (3,700–4,600 ft).



Figure 9. Typical exposure of the lower zone of the lower member of the Lance Formation.

Fox Hills Sandstone (Kfh)

The Fox Hills Sandstone is a poorly exposed buff-colored, white and friable to semi-friable sandstone that was deposited as shoreface sands in the retreating Western Interior Seaway. Tabular to trough cross-bedding is common (fig. 10A); *Ophiomorpha* trace fossils are common to abundant (fig. 10B), while *Gordia?* sp. are rare. Coal beds 0.2–0.9 m (0.5–3 ft) thick are found within a 9 m-thick (30 ft) carbonaceous shale zone just north of Interstate 80 that correlate to the 3 m-thick (10 ft) Nebraska coal zone of Hettinger and others (2008) 5

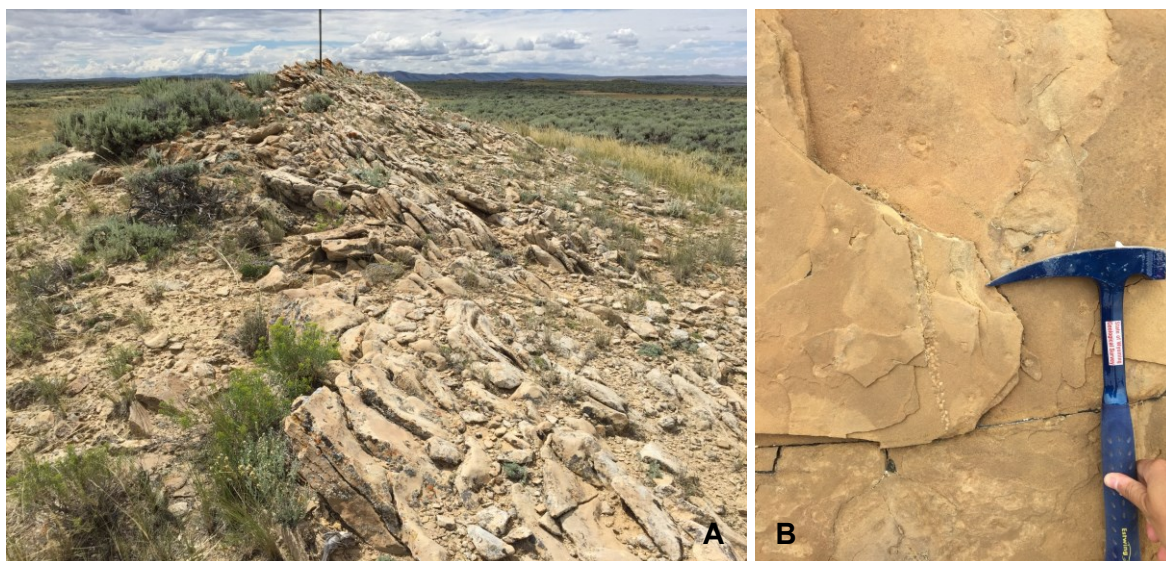


Figure 10. Fox Hills Sandstone showing (A) tabular cross-bedding and (B) *Ophiomorpha* trace fossil.

km (3 mi) southeast of the Rawlins Peak SW quadrangle. The Fox Hills Formation interfingers with both the lower member of the Lance Formation and the Lewis Shale, but this interfingering relationship is not well exposed in the study area. The formation usually erodes to light brown and forms a whitish-yellow soil and vegetated zone that is visible only on satellite imagery. Finn and Johnson (2005) indicate that the Fox Hills Sandstone consists of approximately five individual marginal-marine to coastal sandstones over a 150 m (490 ft) thick zone that interfingers with the Lewis Shale and the Lance Formation. The Fox Hills Sandstone in the study area is approximately 180–195 m (580–640 ft) thick.

Lewis Shale (Kle, Kleu, Kled, Klel)

This valley-forming formation was deposited as marine sediments during the final major transgression and regression of the Late Cretaceous epicontinental sea. The Lewis Shale is considered Maastrichtian at approximately 71 to 69 Ma (Perman, 1987). The formation is composed of shale and sandstone units that interfinger with the overlying Fox Hills Sandstone. Three main facies are identified: nearshore, shelf, and basin marine depositional environments (Perman, 1987). The Lewis Shale was deposited during a north to south progradation. Most of the formation is marine shale, but several upward-coarsening sequences of siltstone and sandstone are interpreted as a prograding sequence of shelf to nearshore deposits.

Lewis Shale (Kle), upper part (Kleu), and Lewis Shale, lower part (Klel): The upper and lower parts of the Lewis Shale are poorly exposed gray to dark-gray shale that weathers light gray to bluish gray (fig. 11). This marine shale is occasionally interbedded with pale yellowish-gray to brown, moderately rounded, very fine grained sandstone bodies that weather rusty brown and orange to light brown. The shale is fissile, contains trace amounts of



Figure 11. Well-exposed outcrop of Lewis Shale.



Figure 12. Bentonite marker bed in the Lewis Shale.

coarser
detritus,
and
displays

no visible bedding. A distinct bentonite marker bed 0.6–0.9 m (2–3 ft) thick was mapped in the upper part of the Lewis Shale (fig. 12), in the central part of the Rawlins Peak SW quadrangle. The lower part of the Lewis Shale is dark gray shale, poorly exposed, and forms valleys. The basal contact is conformable and gradational and mapped above the laterally persistent sandstones of the Almond Formation. The upper part of the Lewis Shale is 210–360 m (690–1,200 ft) thick, the lower part of the Lewis Shale is 250 m (820 ft) thick, and the overall Lewis Shale, including the Dad Sandstone Member, averages approximately 590 m (1,900 ft) thick in the study area.

Dad Sandstone Member (Kled): The Dad Sandstone Member of the Lewis Shale consists of shallow marine sandstone interbedded with shale. The sandstone is concretionary, fine

grained, well sorted, subrounded, light brown, and weathers medium to dark brown (fig. 13). Sandstones are dominantly ripple cross-bedded, contain minor iron oxidization, and locally preserved *Skolithos* trace fossils. Perman (1987) interpreted the Dad Sandstone as the lower delta-front region of the Sheridan Delta (Gill and Cobban, 1973) to the north. It is considered part of a deep basin turbidite system, possibly a down-dip tongue of the Fox Hills Sandstone (Perman 1987; Pyles and Slatt, 2000). The upper contact with the upper Lewis Shale is well exposed in parts of the study area, especially near the boundary between the two maps. Sandstone outcrops are only exposed in valleys on the south-central part of the Rawlins Peak SW quadrangle, and poorly exposed on the Shamrock Hills quadrangle. Where exposed, the member contains approximately ten thin sandy zones approximately 3 m (10 ft) thick, separated by shales 6–10 m (20–33 ft) thick (Gill and others, 1970). The total measured thickness is approximately 90–110 m (290–360 ft), but has been reported up to 220 m (720 ft) (Dames & Moore, 1978).



Figure 13. Outcrop of Dad Sandstone Member of the Lewis Shale.

Mesaverde Group (Kal, Kpr, Kar, Khm)

Almond Formation (Kal)

The Almond Formation contains pale yellowish-gray, orange, and ochre, very fine to fine-grained sandstone interbedded with gray to dark-gray shale, carbonaceous shale, and coal. Sandstone and shale zones are several meters thick and weather in a distinctive striped pattern (fig. 14). At the top of the formation, just below the contact with the overlying Lewis Shale, a laterally continuous 0.3 m (1 ft) thick sandstone bed containing



Figure 14. Distinctive striped outcrop pattern exposed in the Almond Formation.

abundant oyster shells (fig. 15) is approximately 20 m (66 ft) below a distinct laterally continuous sandstone marking the top of the Almond Formation. Discontinuous coals are present in the lower part of the



Figure 15. Oyster shells exposed in a marker bed continuous throughout much of the study area, approximately 20 m (66 ft) below the top of the Almond Formation.

formation with beds up to 1.5 m (5 ft) thick, associated with carbonaceous zones with abundant woody fragments. The base of the formation is gradational and conformable.

The Almond Formation represents a coastal plain environment deposited from 72.36 Ma to 70.4 Ma (Luo and Nummedal, 2010). It interfingers with the Lewis Shale locally as a result of westward marine transgression. The Almond Formation was deposited during a period of overall transgression, but contains numerous transgressive-regressive cycles, intraformational unconformities, and flooding surfaces (Martinsen and others, 1995). This formation represents a series of high-frequency back-stepping sequences associated with the transgression between the Almond and Pine Ridge time interval. The Almond Formation is approximately 180 m (590 ft) thick.

Pine Ridge Sandstone (Kpr)

The Pine Ridge Sandstone is a pale yellowish-gray to white, ridge-forming, cross-bedded sandstone that is very fine to fine grained, well sorted, and subangular to subrounded (fig. 16). Weathered surfaces are light gray to white, with rare honeycomb weathering and iron oxide-stained bedding surfaces, commonly in zones 10–12 m (33–39 ft) thick. Sandstones are interbedded with shale, carbonaceous shale, and rare thin coals. Sand lenses are laterally continuous on the scale of several hundred meters.



Figure 16. Typical Pine Ridge Sandstone outcrop.

The base of the Pine Ridge Sandstone is unconformable and sharp, and denotes a hiatus between deposition of the underlying Allen Ridge Formation and the Pine Ridge Sandstone (Luo and Nummedal, 2010). The Pine Ridge Sandstone is laterally equivalent to the Canyon Creek Member of the Ericson Formation on the Rock Springs uplift. It spans an age from 76.92 Ma to 72.36 Ma. The Pine Ridge Sandstone represents fluvial and alluvial deposition. A regional transgression occurred at the top of the Pine Ridge Sandstone. The formation generally thickens to the north, but is highly variable, ranging 50–100 m (160–330 ft) thick.

Allen Ridge Formation (Kar)

The Allen Ridge Formation is a thick sequence of orange-brown shale and very fine to fine-grained concretionary sandstone lenses interbedded with shale, carbonaceous shale, and coal. The sandstones are well-sorted and well-rounded sub-litharenites with dune-scale tabular and trough cross-bedding, current ripples, and rare thin gravels. Sandstones weather brown to rusty brown and contrast sharply with the light-colored beds of the underlying Haystack Mountains Formation. The non-marine lower half of the formation is well exposed; the shaly upper half is poorly exposed and commonly forms a valley, but laterally contains discrete lenticular sandstones interbedded with shale and carbonaceous shale (fig. 17). The lower part has less than 0.3 m-thick (1 ft) lenticular coal beds, while the upper part has coal up to 0.9 m (3 ft) thick that laterally grades into carbonaceous shale.



Figure 17. Allen Ridge Formation comprises slope on left (west) and valley. The valley in the foreground is primarily shale; valley in the background contains abundant sandstone lenses.

The basal contact with the Haystack Mountains Formation is sharp and conformable (fig. 18). The Allen Ridge Formation is laterally equivalent to the Iles Formation in the southern part of the Greater Green River Basin, and the part of the Ericson Sandstone below the Canyon Creek member on the Rock Springs uplift. It is 77.44 Ma to 73.33 Ma (Luo and Nummedal, 2010). The Allen Ridge Formation represents deposition on a coastal/delta/barrier plain, and is approximately 490 m (1,600 ft) thick.



Figure 18. Contact between the Haystack Mountains Formation (right, east) and Allen Ridge Formation (left, west) is marked at the top of the hill capped by a thin orange sandstone.

Haystack Mountains Formation (Khm)

The Haystack Mountains Formation consists of cliff-forming white, gray, or pale yellowish-brown very fine to fine-grained sandstone interbedded with dark-gray shale (fig. 19). Sandstones are commonly comprised of plane beds, trough cross-beds, and hummocky cross-stratification, with rare trace fossils including possible *Skolithos* and *Thalassinoides*. The formation contains carbonaceous shale up to 1.2 m (4 ft) thick with thin, discontinuous coal beds less than 0.3 m (1 ft) thick, just above the Hatfield Sandstone Member. In the northeast part of the Rawlins Peak SW quadrangle five distinct sandstone ridges and shale valleys (including the Espy Shale, Hatfield Sandstone, and Deep Creek Sandstone) were correlated to measured sections by Roehler (1990). Luo and Nummedal (2010) reported six shoreface sandstone tongues near the Rawlins uplift and suggested that the lower part of the Haystack Mountains Formation was a delta system derived from northern sediment sources. The Hatfield Sandstone forms a ridge 6–24 m (20–80 ft) high. The tan to buff-white sandstone unit is 12 m (39 ft) thick, contains faint bedding and some small cross-bedding, and is bioturbated at the base. The upper contact is placed above Roehler's (1990) uppermost unnamed sandstone member and correlates with Roehler and Hansen's (1989) Rocky Point measured section in T. 22 N., R. 88 W., secs. 19 and 30 ("Big Rocks" on map). The basal contact is placed at the base of Roehler and Hansen's (1989) Deep Creek Sandstone Member, an offshore shelf sand.



Figure 19. Typical landscape showing the Steele Shale in the foreground and a hill comprised of Haystack Mountains Formation sandstones in the background.

As interpreted by Roehler (1990), the Haystack Mountains Formation is interbedded marine shale and offshore marine bar sands, grading upward toward more continental deltaic progradational sandstone facies. The Haystack Mountains Formation in the Rawlins area represents a time interval from 80.64 Ma to 78.47 Ma (Luo and Nummedal, 2010), and a transitional zone of nearshore marine sandstone and offshore marine shale. The lower part of the Haystack Mountains Formation possibly recorded a delta system derived from a sediment source to the north (Luo and Nummedal, 2010). The formation is approximately 400 m (1,300 ft) thick.

Steele Shale (Ks)

The Upper Cretaceous (Campanian) Steele Shale is the oldest formation in the study area, existing as poorly exposed dark-gray marine shale with interbedded light-gray to dark-brown calcareous sandstone that weathers golden brown in color (fig. 20). Outcrop exposures in the upper part of the formation are mostly limited to



Figure 20. Sandstone exposed in the Steele Shale.

sandstone beds that occur as 3–7 cm-thick (1–3 in) plane beds, with occasional black lithic grains, hematite, and potassium feldspar. Glauconitic off-shore sandstones occur in the lower section of the Steele Shale with the most striking example occurring in T. 22 N., R. 88 W., sec. 7, in the southeastern part of the Shamrock hills quadrangle (fig. 20). The sandstones that were observed in the study area are very fine to fine grained with salt and pepper coloring, moderate to well sorted, subrounded to rounded grains, and can exhibit moderate to heavy bioturbation. Possible *Schaubcylindrichnus*? and *Cruziana* trace fossils indicate a shallow marine environment. The Steele Shale is often mapped with the Niobrara Formation in the Rocky Mountains, however no Niobrara Formation was observed within the Rawlins Peak SW and Shamrock Hills quadrangles, and the contact locally has been described as indistinct (Berry, 1960). Dips flatten toward the east in the footwall of the Rawlins uplift décollement, creating a monocline structure just east of the Shamrock Hills quadrangle. The base of the Steele Shale is not exposed in the study area, and the full thickness was not determined. Only the upper 630 m (2,100 ft) of the Steele Shale are exposed on the Rawlins Peak SW quadrangle. Barlow (1959) measured the thickness of the Steele Shale/Niobrara Formation (undifferentiated) west of the Rawlins uplift, citing a thickness of 1,540 m (5,050 ft).

REFERENCES

- Barlow, J.A. Jr, 1953, The geology of the Rawlins uplift, Carbon County, Wyoming: Laramie, University of Wyoming, Ph.D. dissertation, 179 p.
- Barlow, J.A., Jr., 1959, Cretaceous section, west flank of Rawlins uplift, T. 21 N., R. 88 & 89 W., Carbon County, Wyoming, *in* Haun, J.D., and Weimer, R.J., eds., Symposium on Cretaceous rocks of Colorado and adjacent areas: Rocky Mountain Association of Geologists 11th Field Conference Guidebook, Washakie, Sand Wash, and Piceance Basins, p. 110–113.
- Berry, D.W., 1960, Geology and ground-water resources of the Rawlins area, Carbon County, Wyoming: U.S. Geological Survey Water Supply Paper 1458, 74 p., 1 sheet.
- Bilbey, S.A., Trujillo, K.C., Robinson, Peter, Hall, J.E., and Hall, Q.W., 2010, Preliminary and final paleontological evaluation for the Rockies Express/REX Pipeline Project 2004-2006, Wyoming and Colorado, 6 v., >1500 p.
- Carroll, C.J., Ratigan, D.R., Lynds, R.M., and Palkovic, M.J., 2015, Preliminary geologic map of the Rawlins Peak SW quadrangle, Carbon County, Wyoming: Wyoming State Geological Survey Open File Report 15-6, 1 sheet, scale 1:24,000.
- Dames & Moore Co., 1978, Coal resource occurrence and coal development potential maps of the southwest quarter of the Rawlins Peak 15-minute quadrangle, Carbon County, Wyoming: Denver, Colo., U.S. Geological Survey Open-File Report 78-618, 32 p., 18 sheets.
- Dames & Moore Co., 1979, Coal resource occurrence and coal development potential maps of the Riner quadrangle, Carbon and Sweetwater Counties, Wyoming: Denver, Colo., U.S. Geological Survey Open-File Report 79-116, 32 p., 32 sheets.
- Edson, G.M., 1979, Preliminary geologic map and coal sections of the Seaverson Reservoir quadrangle, Carbon County, Wyoming: U.S. Geological Survey Open-File Report 79-1577, scale 1:24,000.
- Finn, T.M., and Johnson, R.C., 2005, Subsurface stratigraphic cross section of Cretaceous and lower Tertiary rocks in the southwestern Wyoming Province, *in* U.S. Geological Survey, Southwestern Wyoming Province Assessment Team, comp., Petroleum systems and geologic assessment of oil and gas in the southwestern Wyoming Province, Wyoming, Colorado, and Utah: U.S. Geological Survey Digital Data Series 69-D, chap. 14, 12 p.
- Folk, R.L., 1980, Petrology of sedimentary rocks: Austin, TX., Hemphill Publishing Company, 182 p.
- Gazin, C.L., 1962, A further study of the lower Eocene mammalian faunas of southwestern Wyoming: Smithsonian Miscellaneous Collections, v. 144, no. 1, 98 p.
- Gehrels, George, 2014, Detrital zircon U-Pb geochronology applied to tectonics: Annual Reviews in Earth and Planetary Sciences, v. 42, p. 127–149.
- Gehrels, George, and Pecha, Mark, 2014, Detrital zircon U-Pb geochronology and Hf isotope geochemistry of Paleozoic and Triassic passive margin strata of western North America: Geosphere, v. 10, p. 49–65.
- Gemmill, C.E.C., and Johnson, K.R., 1997, Paleoecology of a late Paleocene (Tiffanian) megaf flora from the northern Great Divide Basin, Wyoming: Palaios, v. 12, no. 5, p. 439–448.
- Gill, J.R., and Cobban, W.A., 1973, Stratigraphy and geologic history of the Montana Group and equivalent

- rocks, Montana, Wyoming, North and South Dakota: U.S. Geological Survey Professional Paper 776, 37 p.
- Gill, J.R., Merewether, E.A., and Cobban, W.A., 1970, Stratigraphy and nomenclature of some Upper Cretaceous and lower Tertiary rocks in south-central Wyoming: U.S Geological Survey Professional Paper 667, 53 p.
- Gregory, R.W., and Bagdonas, D.A., 2012, Preliminary geologic map of the Separation Rim quadrangle, Carbon County, Wyoming: Wyoming State Geological Survey Open File Report 12-2, 1 sheet, scale 1:24,000.
- Grout, M.A., and Verbeek, E.R., 1992, Joint-history summary and orientation data for Upper Cretaceous sandstones, Rawlins and Rock Springs uplifts, Washakie Basin, southern Wyoming: U.S. Geological Survey Open-File Report 92-388, 30 p.
- Harris, R.E., 2004, Industrial minerals and construction materials map of Wyoming: Wyoming State Geological Survey Map Series 47, 1 sheet, scale 1:500,000.
- Hartman, J.H., Butler, R.D., and Bogan, A.E., 2015, Late Cretaceous brackish and continental mollusks from Black Buttes area of Bitter Creek, Sweetwater County, Wyoming: Wyoming Geological Association 68th Annual Field Conference Guidebook, p. 88-125.
- Hasiotis, S.T., and Honey, J.G., 2000, Paleohydrologic and stratigraphic significance of crayfish burrows in continental deposits: Examples from several Paleocene Laramide Basins in the Rocky Mountains: *Journal of Sedimentary Research*, v. 70, no. 1, p. 127-139.
- Heller, P.L., McMillan, M.E., and Humphrey, Neil, 2011, Climate-induced formation of a closed basin: Great Divide Basin, Wyoming: *Geological Society of America Bulletin*, v. 123, p. 150-157.
- Hettinger, R.D., and Brown, Robert, 1979, Geophysical and lithologic logs of 1977 coal drilling in the Fort Union Formation, Carbon and Sweetwater Counties, Wyoming: U.S. Geological Survey Open-File Report 79-326, 80 p.
- Hettinger, R.D., Honey, J.G., Ellis, M.S., Barclay, C.S.V., and East, J.A., 2008, Geologic map of the Upper Cretaceous and Tertiary strata and coal stratigraphy of the Paleocene Fort Union Formation, Rawlins-Little Snake River area, south-central Wyoming: U.S. Geological Survey Scientific Investigations Map 3053, 3 sheets.
- Hettinger, R.D., Honey, J.G., and Nichols, D.J., 1991, Chart showing correlations of Upper Cretaceous Fox Hills Sandstone and Lance Formation, and lower Tertiary Fort Union, Wasatch, and Green River Formations, from the eastern flank of the Washakie Basin to the southeastern part of the Great Divide Basin, Wyoming: U.S. Geological Survey Miscellaneous Investigations Series Map I-2151, 1 sheet.
- Hettinger, R.D., and Kirschbaum, M.A., 1991, Chart showing correlations of some Upper Cretaceous and lower Tertiary rocks, from the east flank of the Washakie Basin to the east flank of the Rock Springs uplift, Wyoming: U.S. Geological Survey Miscellaneous Investigations Series Map I-2152, 1 sheet.
- Honey, J.G., and Hettinger, R.D., 2004, Geologic map of the Peach Orchard Flat quadrangle, Carbon County, Wyoming, and descriptions of new stratigraphic units in the Upper Cretaceous Lance Formation and Paleocene Fort Union Formation, eastern Greater Green River Basin, Wyoming-Colorado: U.S. Geological Survey Scientific Investigations Map 2835, 2 sheets.
- Krampert, E.W., 1951, Bell Springs field: South-central Wyoming, Wyoming Geological Association 6th

- Annual Field Conference Guidebook, p. 117.
- Lillegraven, J.A., 2015, Late Laramide tectonic fragmentation of the eastern Greater Green River Basin, Wyoming: *Rocky Mountain Geology*, v. 50, no. 1, p. 30–118.
- Luo, Hongjun, and Nummedal, Dag, 2010, Late Cretaceous stratigraphy and tectonics across southwestern Wyoming: *The Mountain Geologist*, v. 47, no. 3, p. 91–116.
- Lynds, R.M., and Carroll, C.J., 2015, Stratigraphic cross sections and subsurface model of the Lance and Fort Union Formations, Great Divide Basin, Wyoming: Wyoming State Geological Survey Open File Report 15-3, 1 sheet.
- Lynds, R.M., Palkovic, M.J., Carroll, C.J., and Ratigan, D.R., 2015, Preliminary geologic map of the Shamrock Hills quadrangle, Carbon County, Wyoming: Wyoming State Geological Survey Open File Report 15-6, 1 sheet, scale 1:24,000.
- Marrs, R.M., and Grasso, D.N., 1991, Geologic applications of remote sensing and GIOS: A Wyoming landscape perspective, *in* Snoke, A.W., Steidtmann, J.R., and Roberts, S.M., eds., *Geology of Wyoming: Geological Survey of Wyoming [Wyoming State Geological Survey] Memoir 5*, v. 2, p. 790–815.
- Martinsen, R.S., Christiansen, G.E., Olson, M.A., and Surdam, R.C., 1995, Stratigraphy and lithofacies of the Almond Formation, Washakie and Great Divide Basins, Wyoming, *in* Jones, R.W., and Winter, G.A., eds., *Resources of southwestern Wyoming: Wyoming Geological Association 6th Annual Field Conference Guidebook*, p. 297–310, 2 sheets.
- Martner, B.E., and Marwitz, J.D., 1982, Wind characteristics in southern Wyoming: *Journal of Applied Meteorology*, v. 21, p. 1815–1827.
- Masursky, Harold, 1962, Uranium-bearing coal in the eastern part of the Red Desert area, Wyoming: U.S. Geological Survey Bulletin 1099-B, 152 p., 10 sheets.
- McComas, Katie, 2014, A new Puercan *Arctocyonid* genus from the Great Divide Basin, Wyoming: Boulder, University of Colorado, M.S. thesis, 56 p.
- McLaughlin, J.F., and Fruhwirth, Jeff, 2008, Preliminary geologic map of the Rawlins 30' x 60' quadrangle, Carbon and Sweetwater Counties, Wyoming: Wyoming State Geological Survey Open File Report 8-4, 1 sheet, scale 1:100,000.
- Nichols, D.J., and Ott, H.L., 1978, Biostratigraphy and evolution of the *Momipites-Caryapollenites* lineage in the early Tertiary in the Wind River Basin, Wyoming: *Palynology*, v. 2, p. 94–112.
- Otteman, A.S., and Snoke, A.W., 2005, Structural analysis of a Laramide, basement-involved, foreland fault zone, Rawlins uplift, south-central Wyoming: *Rocky Mountain Geology*, v. 40, p. 65–89.
- Perman, R.C., 1987, Deltaic deposits of the Upper Cretaceous Dad Sandstone Member of the Lewis Shale, south-central Wyoming: *Rocky Mountain Association of Geologists*, v. 24, no. 1, p. 10–18.
- Pipiringos, G.N., 1955, Tertiary rocks in the central part of the Great Divide Basin, Sweetwater County, Wyoming. *in* Camp, R.J., chairman, *Green River Basin: Wyoming Geological Association 10th Annual Field Conference Guidebook*, p. 100–104.
- Pipiringos, G.N., 1961, Uranium-bearing coal in the central part of the Red Desert area, Wyoming: U.S. Geological Survey Bulletin 1099-A, 104 p, 5 sheets.
- Pyles, D.R., and Slatt, R.M., 2000, A high-frequency sequence stratigraphic framework for shallow through

- deep-water deposits of the Lewis Shale and Fox Hills Sandstone, Great Divide and Washakie Basins, Wyoming, *in* Weimer, P., Slatt, R.M., Coleman, J., Rosen, N.C., Nelson, H., Bouma, A.H., Styzen, M.J., and Lawrence, D.T., eds., *Deep-water reservoirs of the world: Gulf Coast Section Society of Economic Paleontologists and Mineralogists Foundation, 20th annual Bob F. Perkins Research Conference*, Houston, Texas, December 3-6, 2000, p. 836–861.
- Rigby, J.K., Jr., 1980, Swain Quarry of the Fort Union Formation, middle Paleocene (Torrejonian), Carbon County, Wyoming—geologic setting mammalian fauna: *Evolutionary Monographs*, v. 3, 179 p.
- Rocky Mountain Energy Co., 2014, Unpublished stratigraphic data from coal exploration wells drilled in the eastern Great Divide Basin: Data provided through a cooperative agreement with the U.S. Geological Survey, Anadarko Corporation and the Wyoming State Geological Survey.
- Roehler, H.W., 1990, Stratigraphy of the Mesaverde Group in the central and eastern Greater Green River Basin, Wyoming, Colorado, and Utah: U.S. Geological Survey Professional Paper 1508, 52 p., 2 sheets.
- Roehler, H.W., and Hansen, D.E., 1989, Surface and subsurface correlations showing depositional environments of the Upper Cretaceous Mesaverde Group and associated formations, Lost Soldier Field to Cow Creek, southwest Wyoming: U.S. Geological Survey Miscellaneous Field Studies Map MF-2076, 1 sheet.
- Sanders, R.B., 1974, Geologic map and coal resources of the Riner quadrangle, Carbon and Sweetwater Counties, Wyoming: U.S. Geological Survey Coal Investigations Map 68, 1 sheet, scale 1:24,000.
- Sanders, R.B., 1975, Geologic map and coal resources of the Creston Junction quadrangle, Carbon and Sweetwater Counties, Wyoming: U.S. Geological Survey Coal Investigations Map 73, 1 sheet, scale 1:24,000.
- Saracino, A.M., 1984, Sedimentology and petrology of the Fort Union Formation: Fort Collins, Colorado State University, M.S. thesis, 154 p.
- Tyler, Roger, Kaiser, W.R., Scott, A.R., Hamilton, D.S., and Ambrose, W.A., 1995, Geologic and hydrologic assessment of natural gas from coal—Greater Green River, Piceance, Powder River, and Raton Basins, western United States: Austin, Texas, Bureau of Economic Geology Report of Investigations No. 228, 219 p.
- U.S. Geological Survey, 2015, National Coal Resource Data System (NCRDS) website of stratigraphic coal resource data: <http://energy.usgs.gov/Tools/NationalCoalResourceDataSystem.aspx>, accessed 09/01/2015.
- WOGCC, 2015, Wyoming Oil and Gas Conservation Commission website, at <http://wogcc.state.wy.us/>, accessed 08/14/2015.

APPENDIX A: DETRITAL ZIRCON GEOCHRONOLOGY

Detrital zircon geochronology analyses were conducted at the University of Arizona LaserChron Center using methods described by Gehrels and Pecha (2014). Zircons from eight samples in the study were analyzed for their ratios of $^{206}\text{Pb}/^{238}\text{U}$ and $^{206}\text{Pb}/^{207}\text{Pb}$ to determine the age of each zircon. The ratio of $^{207}\text{Pb}/^{235}\text{U}$ was then calculated from the aforementioned ratios and the known value of $^{238}\text{U}/^{235}\text{U}$ ($^{238}\text{U}/^{235}\text{U} = 137.82$; Gehrels, 2014). Samples were analyzed on a Nu Plasma multicollector ICP-MS coupled to a Photon Machines Analyte G2 excimer laser ablation system. The Haystack Mountains Formation, Pine Ridge Formation, Lance Formation (lower member and Red Rim Member), Fort Union Formation (China Butte and Overland Members), and Battle Spring Formation yielded detrital zircons for this study (Table A1). Descriptions (figs. A1–A8) and point counts (fig. A9) were performed on thin sections from corresponding samples. U-Pb age data are available from the Wyoming State Geological Survey upon request.

Table A1. Samples processed for detrital zircon U-Pb age dates. Latitude and longitude values are in GCS NAD27, and n represents the number of zircons analyzed for each sample.

Sample ID	Latitude	Longitude	Formation	n
GGRB-14-24	41.95075	-107.47787	Tbs	301
GGRB-14-23	41.78912	-107.47989	Tfo	292
GGRB-14-17	41.85050	-107.44489	Tfo	299
GGRB-14-21	41.78946	-107.39742	Tfc	270
GGRB-14-14	41.85015	-107.42533	Klr	279
GGRB-14-27	41.81369	-107.39332	Kll	192
GGRB-14-20	41.96387	-107.43463	Kpr	299
GGRB-14-19	41.98944	-107.43187	Khm	297

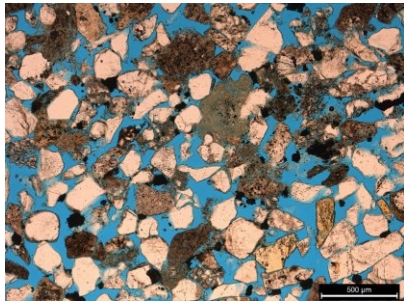


Figure A1. Thin section photomicrograph of sample GGRB-14-24 from the Battle Spring Formation. Medium-grained, subangular, moderately sorted, feldspathic/lithic arenite with high porosity. Feldspar grains have commonly altered to clay, with some detrital clay present as well.

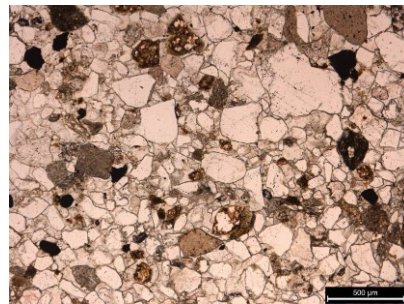


Figure A2. Thin section photomicrograph of sample GGRB-14-23 from the Overland Member of the Fort Union Formation. Very fine grained, subangular to subrounded, moderately well sorted sublitharenite. The sample has very low porosity, due to the abundant calcite cement that binds the detrital framework. Quartz grains are dominantly monocrystalline.

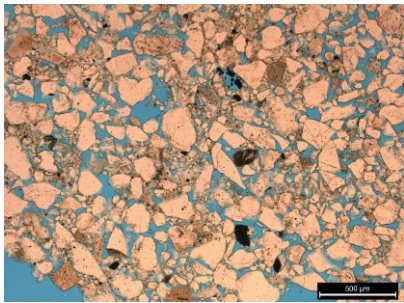


Figure A3. Thin section photomicrograph of sample GGRB-14-17 from the Overland Member of the Fort Union Formation. Very fine grained, subrounded, moderately sorted sublitharenite. As opposed to GGRB-14-23, this sample is less indurated and has higher porosity.

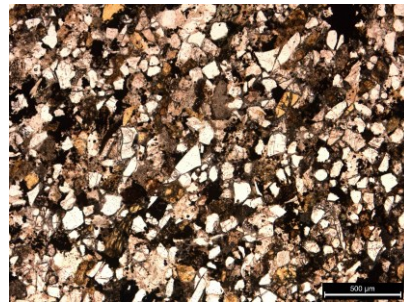


Figure A4. Thin section photomicrograph of sample GGRB-14-21 from the China Butte Member of the Fort Union Formation. Very fine grained, subrounded, moderately sorted lithic wacke. Clay and hematite occlude most pore throats, resulting in a well-lithified sample with very low porosity.

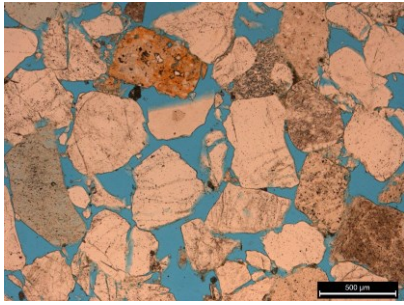


Figure A5. Thin section photomicrograph of sample GGRB-14-14 from the Red Rim Member of the Lance Formation. Medium- to coarse-grained, subangular to subrounded, well-sorted litharenite. This sample has high porosity and contains an abundance of chert grains and lithic fragments. Some quartz grains are polycrystalline.

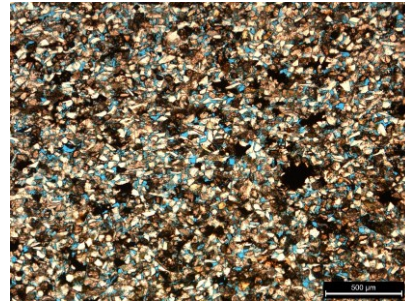


Figure A6. Thin section photomicrograph of sample GGRB-14-27 from the lower member of the Lance Formation. Grains are silt sized to very fine grained sand, angular and well sorted. Composition is arkose wacke, with high porosity despite the fine grain size. Contains an abundance of clay and K-feldspar.

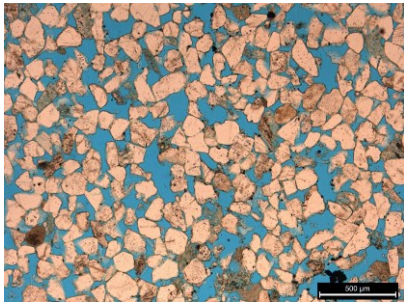


Figure A7. Thin section photomicrograph of sample GGRB-14-19 from the Haystack Mountains Formation. Very fine grained, subangular, well-sorted sublitharenite, with very high porosity and a considerable amount of chert. Intragranular dissolution is common.

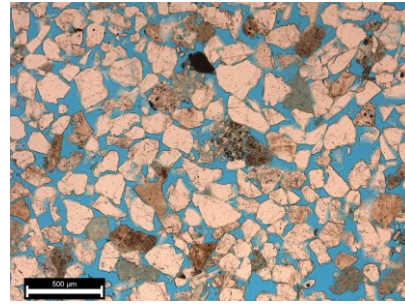


Figure A8. Thin section photomicrograph of sample GGRB 14-20 from the Pine Ridge Sandstone. Fine-grained, subangular to subrounded, well-sorted sublitharenite with high porosity.

APPENDIX B: PALYNOLOGY

Previous Investigations

The U.S. Geological Survey conducted palynology and fossil studies from Cretaceous and Paleocene rocks south of I-80. Hettinger and others (1991) collected several samples near the Cretaceous-Paleogene (K-Pg; formerly Cretaceous-Tertiary or K/T) boundary. Palynology results from that work indicate the upper part of the Lance Formation is bracketed between Maastrichtian to early Paleocene in age, and contains the K-Pg boundary zone. However, the latest Maastrichtian pollen species *Wodehouseia* assemblage is missing, suggesting that the K-Pg boundary is an unconformity along the Atlantic Rim.

Pollen analyses from Hettinger and others (1991) show that the K-Pg boundary resides somewhere near the upper third of the Red Rim Member of the Lance Formation (their “Unnamed Cretaceous and Tertiary sandstone unit”). They found predominately late Maastrichtian palynomorphs in the lower part of the Red Rim Member, while the upper Red Rim Member contained several samples with early Paleocene palynomorph assemblages. Within the overlying China Butte Member of the Fort Union Formation (their “Fort Union Formation”), they found palynomorph assemblages characteristic of early Paleocene. Their China Butte Member samples were collected from the lower part of the section, near the Red Rim coal zone. They also sampled the Overland Member (their “Unnamed upper Paleocene unit”) and found middle to late Paleocene palynomorph assemblages.

The nomenclature of Nichols and Ott (1978) indicates that Lance and Fort Union Formation polymorphs of the Atlantic Rim and Rawlins uplift span the range of P6 (youngest) to P2 (oldest). However, Lillegraven (2015) suggests that this system is controlled more by paleoenvironmental constraints than discrete parts of geologic time. Thus, pollen assemblages collected in this area represent a relative range of geologic time.

Correspondingly, several authors also identified vertebrate fossils south of the study area. Rigby (1980) found early Paleocene (Torrejonian) mammal fossils in the Swain Quarry of the upper China Butte Member of the Fort Union Formation. McComas (2014) discovered a new genus and species of earliest Paleocene *Arctocyonid* just a few kilometers south of the Rawlins Peak SW quadrangle. The fossils suggest that the lowest part of the China Butte Member (below the Red Rim and Daley Ranch coal zones) is early Puercan in age. These are correlative to zone P2 of Nichols and Ott (1978) and the Continental Divide coal zone of Hettinger and others (2008). In the upper Wasatch Formation, at the Dad fossil vertebrate locality, Gazin (1962) found early Eocene (late Wasatchian) fossils. Nearby, Hettinger and others (1991) also found early Eocene (late Wasatchian) fossils in the upper Wasatch Formation.

Methods

Coal and carbonaceous shale samples were collected from the Fort Union, Lance, Almond, Pine Ridge, and Haystack Mountains Formations in the study area, and from the Wasatch Formation west of the study area. Coal roof or floor rock, usually carbonaceous shale, were targeted for sampling, in hope of selecting the best palynomorphs because pollen in coal beds are usually too bioturbated for recovery. Twelve samples were sent to Biostratigraphy.com (Garland, TX) for processing and analysis. In addition to age, the palynology samples were used to determine paleoenvironment based on the taxa identified, and thermal maturity based on spore color. Samples are detailed in Table B1; sample locations are identified on the maps.

Results

Age

Table B1 shows the range of possible ages for each sample. Two samples were collected from the Haystack Mountains Formation, including CC 92 from the middle of the formation, and CC 120 from the top of the formation. The former sample is undifferentiated Campanian to late Campanian; the latter sample is middle to late Campanian, suggesting the Haystack Mountain Formation is middle to late Campanian. For the Pine Ridge Sandstone, one sample, CC 94, indicates a pollen estimated age of late Campanian.

The Lance Formation is estimated as early to late Maastrichtian, but not latest Maastrichtian. Sample CC 80 was collected from the middle of the lower member of the Lance Formation, and is late Campanian to early Maastrichtian in age. Because Hettinger and others (1991) estimate that the lower member of the Lance Formation is Maastrichtian, CC 80 is most likely early Maastrichtian, rather than late Campanian. Sample CC 88 was taken from the upper part of the Red Rim Member, and is late Maastrichtian. This study was not able to identify the exact K-Pg boundary but observed that it is stratigraphically higher than sample CC 88, and lower than the base of the Fort Union Formation at that location on the map. This study also noted that *Wodehouseia* does not occur in any of the WSGS study area samples, indicating a gap in time at the K-Pg boundary.

The Fort Union Formation samples imply an age of early to late Paleocene, in general agreement with Hettinger and others (1991). Sample CC 112 was collected from the upper part of the China Butte Member, and is early Paleocene age. Sample GGRB-FU-3 was collected from the Fort Union Formation, and is late Paleocene age. From two samples collected west of the map area the lowest Wasatch Formation coal zones are early Eocene in age (not listed on table B1).

Four samples did not contain enough palynomorphs to determine age, listed in the results table. In addition, six samples had age estimates that were erroneously young. For example, several Fort Union samples gave early Eocene ages. Presumably these errors come from limitations in palynomorph age determination and a lack of preserved pollen in coal samples.

Paleoenvironment

These palynology paleoenvironment results generally agree with the interpretations of Hettinger and others (2008) and Roehler (1990). The Haystack Mountains Formation contains both marine palynomorphs and fluvial/floodplain palynomorphs in the Hatfield Sandstone, suggesting the Haystack Mountains Formation represents a range of environments. The shales were deposited in marine environments, and the thick, laterally extensive sandstones such as the Deep Creek and Hatfield Sandstones represent shoreline regressions. The Pine Ridge Sandstone is terrestrial fluvial/floodplain, consistent with Roehler's (1990) interpretation of a highland, alluvial-plain environment.

The lower member of the Lance Formation was paludal-lacustrine, and the Red Rim Member of the Lance Formation was fluvial/floodplain. The Red Rim Member represents a change from the coal-mired coastal plain environment of the lower member to an alluvial-plain landscape. The China Butte Member of the Fort Union Formation was a paludal-lacustrine environment, similar to Roehler's (1990) interpretation.

Table B1. Results for palynology analyses showing sample name, unit sampled, palynology age, paleoenvironment, thermal maturity (as estimated percent Ro, vitrinite reflectance), and sample location (latitude and longitude in GCS NAD27). Blank spaces for age and vitrinite reflectance indicate the palynomorph count was too low to make a determination. Paleoenvironment was not determined for some samples.

Sample ID	Unit	Age (this report)	Prev. Age Estimate (Hettinger and others, 1991)	Paleoenvironment	est. %Ro	Latitude	Longitude
CC 112	Tfo/Tfc contact	Early Paleocene	Early Paleocene	Paludal-lacustrine	0.32	41.90669	-107.46967
CC 88	Klr	Late Maastrichtian	Late Maastrichtian-Early Paleocene	Fluvial, floodplain	0.4	41.77873	-107.38935
CC 80	Kll	Late Campanian - Early Maastrichtian	Maastrichtian	Paludal-lacustrine	0.4	41.85593	-107.41509
CC 94	Kpr	Late Campanian	--	Fluvial, floodplain	0.4	41.96381	-107.43461
CC 92	Khm, Hatfield Sandstone Member	Campanian undiff. - Late Campanian	--	Marine	0.4	41.98961	-107.43001
CC 120	Khm, near top	Middle Campanian - Late Campanian	--	Nearshore marginal marine	0.4	41.8573	-107.38558
GGRB-FU-1	Tfc, Hadsell Draw coal	N/A	Early Paleocene	Paludal-lacustrine coal mire	--	41.79835	-107.4047
GGRB-FU-2	Tfc, Olson Draw coal	N/A	Early Paleocene	Paludal-lacustrine coal mire	--	41.78373	-107.40025
GGRB-FU-3	Tfc, Lower Olson Draw coal	Late Paleocene	Early Paleocene	Paludal-lacustrine coal mire	0.4	41.78339	-107.39971
GGRB-FU-4	Tfc, Lower Olson Draw coal	N/A	Early Paleocene	Paludal-lacustrine coal mire	--	41.78231	-107.39879
GGRB-FU-5	Tfc, Hadsell Draw coal	N/A	Early Paleocene	Paludal-lacustrine coal mire	--	41.78128	-107.39827
GGRB 14-4	Klr	Late Maastrichtian	Late Maastrichtian-Early Paleocene	Fluvial, floodplain	0.4	41.682436	-107.47764

APPENDIX C: COAL QUALITY

Fifteen coal and carbonaceous shale samples were analyzed by Wyoming Analytical Laboratories Inc., Laramie, Wyoming for proximate and ultimate analyses, equilibrium moisture, and mercury. Results were displayed on an as-received, moisture-free, and moisture- and ash-free basis. Displayed heat values are lower than expected because they were collected from weathered outcrop material. Many of the samples resemble low values due to the nature of the rock sampled. Most of the samples are coal in-seam, but others are carbonaceous shale associated with coal beds (such as CC358). The average mercury in coal sampled is 0.051 mg/kg, or 51 ppb. These samples were entered into the U.S. Geological Survey's National Coal Resource Data System (NCRDS) (U.S. Geological Survey, 2015) by WSGS during this mapping project.

Table C1. Coal quality sample results collected from the study area. Sample locations are given as latitude and longitude in GCS NAD27.

Sample ID	Sample Description	Latitude	Longitude	Moisture Content	EQ. Moist	Ash Content		Volatile Matter		
				Total	Wt.%	As Received		As Received		MAF
				As Rec. %		%	Dry	%	Dry	
				%			%		%	
1125CC-B	Tfc, Hadsell Draw shaly coal	41.79336	-107.40136	25.4	21.6	7.4	9.9	30.4	40.7	45.2
1125CC-C*	Tfc, Muddy Creek carb. shale	41.79145	-107.40602	41.9	37.6	25.9	44.6	18.9	32.4	58.5
1125CC-D	Tfc, Chicken Springs #2 coal	41.78961	-107.40920	39.1	34.0	7.0	11.4	30.1	49.4	55.8
1125EC-E	Tfc, Lower Olson Draw coal	41.80584	-107.41057	41.8	34.8	6.2	10.7	28.1	48.2	54.0
1125EC-F	Tfc, Hadsell Draw coal	41.79904	-107.40582	32.7	29.0	3.7	5.5	30.6	45.5	48.2
1125EC-H	Tfc, Riner coal	41.77985	-107.40505	28.9	25.4	14.0	19.6	11.8	16.6	20.7
CC98A	Tfc, Lower Olson Draw coal	41.78854	-107.39742	21.2	12.3	13.6	41.0	45.3	52.4	37.3
CC138A	Tfc, Upper Separation Creek coal	41.79909	-107.40993	11.8	1.9	2.1	37.3	40.9	41.7	52.0
DR15-193	Tfc, Hadsell Draw coal	41.76265	-107.41085	11.8	--	10.8	12.3	40.0	45.3	51.7
CC-338	Kal, uppermost coal	41.85301	-107.39304	12.2	--	10.3	11.7	39.2	44.7	50.6
DR15-190	Tfc, Hadsell Draw coal	41.83788	-107.42627	12.3	--	15.7	18.0	38.2	43.6	53.1
DR15-191	Tfc, Olson Draw coal	41.83047	-107.42407	11.8	--	6.1	6.9	36.5	41.4	44.5
CC-138B	Tfc, Muddy Creek coal	41.79912	-107.40978	12.7	--	1.9	2.2	36.7	42.0	43.0
CC-98B	Tfc, Hadsell Draw/Red Rim coal	41.78854	-107.39744	19.7	--	13.4	16.7	34.9	43.4	52.1
CC358*	Tfc, Olson Draw carb shale #6	41.83019	-107.42399	--	--	92.9	94.1	4.9	5.0	84.0
Average				21.6	22.7	8.6	15.6	34.1	42.7	46.8

*carbonaceous shale not in average

Table C1. continued

Sample ID	Fixed Carbon			Sulfur Content			Heating Values (BTU)			Carbon		
	As Received	Dry	MAF	As Received	Dry	MAF	As Received	Dry	MAF	As Received	Dry	MAF
	%	%	%	%	%	%	%	%	%	%	%	%
1125CC-B	36.8	49.4	54.8	0.2	0.2	0.3	7,596	10,181	11,303	46.2	61.9	68.7
1125CC-C*	13.4	23.0	41.5	0.3	0.5	0.9	2,930	5,038	9,091	19.0	32.7	59.0
1125CC-D	23.8	39.1	44.2	0.5	0.8	0.9	5,004	8,211	9,272	33.0	54.1	61.1
1125EC-E	23.9	41.1	46.0	0.2	0.3	0.3	4,862	8,354	9,349	31.8	54.6	61.1
1125EC-F	32.9	48.9	51.8	0.1	0.1	0.1	6,626	9,852	10,430	41.6	61.8	65.4
1125EC-H	45.3	63.8	79.3	0.3	0.4	0.5	7,262	10,215	12,713	47.7	67.1	83.5
CC98A	41.2	47.6	0.4	0.4	0.5	--	7,842	8,649	10,006	44.1	55.9	64.7
CC138A	57.0	58.3	0.2	0.3	0.3	--	10,662	11,692	11,942	60.6	68.7	70.2
DR15-193	37.4	42.4	48.3	0.3	0.3	0.3	7,671	8,692	9,907	54.7	61.9	70.6
CC-338	38.3	43.6	49.4	0.5	0.6	0.6	7,589	8,643	9,792	54.6	62.2	70.4
DR15-190	33.7	38.4	46.9	0.4	0.4	0.5	6,694	7,634	9,304	50.3	57.3	69.9
DR15-191	45.5	51.6	55.5	0.1	0.2	0.2	9,185	10,417	11,193	61.3	69.5	74.7
CC-138B	48.7	55.8	57.0	0.2	0.3	0.3	9,637	11,041	11,284	62.9	72.1	73.7
CC-98B	32.0	39.9	47.9	0.3	0.4	0.5	6,460	8,047	9,662	47.3	58.9	70.8
CC358*	0.9	0.9	16.0	--	--	--	500	500	500	4.3	4.3	73.4
Average	38.2	47.7	44.7	0.3	0.4	0.4	7,468	9,356	10,474	48.9	62.0	69.6

*carbonaceous shale not in average

Table C1. continued

Sample ID	Hydrogen			Nitrogen			Oxygen			Mercury
	As Received	Dry	MAF	As Received	Dry	MAF	As Received	Dry	MAF	mg/kg
	%	%	%	%	%	%	%	%	%	
1125CC-B	2.2	3.0	3.3	0.5	0.7	0.7	18.2	24.3	27.0	--
1125CC-C*	1.1	1.8	3.3	0.4	0.7	1.2	11.5	19.7	35.6	--
1125CC-D	1.5	2.4	2.7	0.7	1.1	1.3	18.4	30.2	34.1	--
1125EC-E	1.4	2.3	2.6	0.4	0.7	0.8	18.3	31.5	35.2	--
1125EC-F	1.9	2.9	3.0	0.5	0.7	0.8	19.5	29.0	30.7	--
1125EC-H	0.7	0.9	1.2	0.9	1.2	1.5	7.6	10.7	13.4	--
CC98A	2.5	3.2	3.7	0.8	1.0	1.1	20.5	26.0	30.1	0.032
CC138A	3.9	4.5	4.6	0.7	0.7	0.8	21.0	23.8	24.3	0.040
DR15-193	1.9	2.1	2.4	1.1	1.2	1.4	19.6	22.2	25.3	0.062
CC-338	1.7	2.0	2.2	2.0	2.3	2.6	18.7	21.3	24.2	0.063
DR15-190	1.5	1.7	2.0	1.2	1.4	1.7	18.6	21.2	25.9	0.055
DR15-191	2.4	2.7	2.9	0.9	1.0	1.1	17.4	19.8	21.2	--
CC-138B	2.9	3.3	3.4	0.8	0.9	0.9	18.6	21.3	21.7	--
CC-98B	1.5	1.9	2.3	0.9	1.1	1.3	16.9	21.0	25.2	0.055
CC358*	0.0	0.0	0.5	0.0	0.0	1.3	1.7	1.7	8.4	0.050
Average	1.8	2.3	2.6	0.8	1.0	1.2	16.8	21.7	24.8	0.051

*carbonaceous shale not in average